AIAA JOURNAL
Vol. 32, No. 12, December 1994

Probability of Failure and Risk Assessment of Structure with Fatigue Cracks

M.-H. Herman Shen* and Minsheng Shen†
Ohio State University, Columbus, Ohio 43210

A methodology is proposed for the evaluation of the reliability of a cracked structure with uncertainties in external loadings, material properties, and initial crack geometry. The methodology consists of determining the probabilistic crack path and calculating the cumulative probability of failure for mixed-mode crack propagation. The performance of the methodology is demonstrated by mode I and mixed-mode fatigue crack problems.

Nomenclature

a	= crack length
a_i	= initial crack length
C	= fatigue material property
d	= displacement
E	= Young's modulus
$g(X)$	= performance function
K_{I}	= mode I stress intensity factor
K_{II}	= mode II stress intensity factor
L	= length of model
$N(X)$	= fatigue life
N_0	= expected life
n	= fatigue material property
p_f	= probability of failure
u_i	= reduced random variable
W	= width of model
X_i	= random variable
X	= random variable vector
β	= reliability index
$\Delta K(a)_{\mathrm{eq}}$	= equivalent stress intensity factor range
θ	= fatigue crack propagation direction
Φ	= standard normal cumulative distribution function

Introduction

MANY optimum or lightweight designed load-carrying structural systems such as turbines, generators, motors, aircraft, and spacecraft are usually under severe operational conditions. One factor of damage that could lead to failure of the system if undetected is a cracking structural member of the system. For example, the Aloha Boeing 737 accident that occurred on April 28, 1988 triggered an awareness of the fact that fatigue damage of in service aircraft structural components is a serious issue that we must deal with immediately.

Extensive research have been done analytically as well as experimentally on the mechanics of fatigue crack growth and the prediction of the crack path of structural components. Almost all of the studies so far were conducted using deterministic mode I fracture analysis methods, in which loading, initial crack conditions, and crack path are assumed known. However, it is clearly indicated in practical applications that fatigue crack growth is sensitive to a variety of complex cyclic loading conditions and initial crack geometry which usually cannot be determined accurately. Most of them are quantifiable only as best engineering estimates. Therefore, the deterministic analysis methods are not sufficient to properly design the critical components in aerospace, mechanical, and civil structures, and flight vehicle structural systems, in particular. To predict the service life of the structural components containing cracks as well as its fracture and risk assessment, in addition to an accurate deterministic analysis procedure, a reliability analysis is also required to account for all of the random uncertainties in the mechanical cyclic loads, material properties, structural forms, and initial crack geometry. This motivates the recent research efforts for the development of the reliability methods to evaluate probability of brittle fracture and to assess the associated risk of engineering components containing flaws.

The probabilistic structural analysis methods[1] (PSAM) have been developed by NASA Lewis Research Center to predicate the effects of uncertainties in loading, material properties, boundary conditions, and geometry on the flight vehicles' structural performances. One of the major tasks under the PSAM project was the development of a nonlinear evaluation of stochastic structures under stress (NESSUS), a probabilistic structural analysis computer code, which integrates finite element methods and probabilistic algorithms.[2] This code is designed for calculating the structural responses (stress, buckling loads, natural frequency, etc.) under uncertainties in analytical models such as propulsion structural components.[3]

Recently, NESSUS has been extended for determining structural reliability considering progressive fracture[4] with a predefined crack path. However, when the crack path is unknown the reliability analysis was not achieved due to the major difficulty of determining the crack growth direction as well as the crack path in progressive fracture.

Another contribution to the reliability analysis of structures under progressive fracture is the recent work of Liu et al.[5] and Besterfield et al.,[6,7] who presented a fusion method of the probabilistic finite element method (PFEM) and reliability analysis for probabilistic fatigue crack growth. Their approach consists of calculating the reliability index via an optimization procedure which is subject to the equality constraints originating from the crack growth direction law and equilibrium, and inequality constraint (i.e., the performance function). The random variable vector includes initial and final crack length, crack angle, crack position, material properties, and external loads. They discretized the unknown crack path into many pieces of straight lines connected at each discretization point. The directions of these straight lines were determined by the crack direction law. However, the performance of the method was demonstrated on mode I fatigue problems only. Consequently, similar to the examples presented by Millwater et al.[4] due to mode I behavior, the fatigue crack growth was restricted in a straight line.

In summary, in all of the studies mentioned[1-7] the crack path (a straight line) was actually predefined, and a cured crack path problem (mixed mode fracture) was considered but has not been studied at all untill recent work by Lua et al.[8,9] In their studies, an efficient stochastic boundary element method was developed to study probabilistic fatigue crack growth under mixed-mode (modes I, II) failure. However, dealing with similar problems via finite element methods has not been shown yet.

Received Oct. 11, 1993; revision received July 7, 1994; accepted for publication July 14, 1994.

*Assistant Professor, Department of Aeronautical and Astronautical Engineering. Member AIAA.

†Graduate Research Assistant, Department of Aeronautical and Astronautical Engineering. Student Member AIAA.

Compared to the mode I problem, the mixed-mode fatigue crack growth reliability problem is more complicated. The major difference is the determination of the crack path which usually is a curve constructed by the information of the primary random variables: external loads, material properties, structure configuration, initial crack geometry, crack position, and other factors.

The goal of this study is to develop a method of computing the fatigue crack growth path and the cumulative probability of failure for mixed-mode crack propagation. Two basic issues are addressed in this study. First, a new methodology to determine the probabilistic crack path of mixed mode is presented. Second, the cumulative probability associated with the crack path, a straight line or a cure, is calculated by the fast probability integration (FPI) technique.

Theoretical Formulations

Review of Fast Probability Integration Technique

In general, a structural reliability analysis is needed to compute the probability of failure which usually requires a multiple integration. Except in the cases of one or two random design factors, it is a practical impossibility; therefore, analytical approximation methods are needed. Since the 1970s, a number of numerical methods have been developed to describe structural reliability without having to perform the computational intensive multiple integration. For example, the FPI technique, an advanced reliability method, was designed to generate a reliable distribution function in much less computing time than that for Monte Carilo simulation. Therefore, in this research, all of the reliability calculations were performed using a NESSUS/FPI module.

In structural reliability analysis, a performance function or limit state function $g(\boldsymbol{X})$ needs to be defined in terms of a vector of basic design factors, $X = (X_1, X_2, \ldots, X_n)^T$, such that the probability of failure is

$$p_f = P[g(\boldsymbol{X}) \leq 0] \tag{1}$$

In this study, the performance function is defined as

$$g(\boldsymbol{X}) = N(\boldsymbol{X}) - N_0 \tag{2}$$

$N(\boldsymbol{X})$ and N_0 are the service life and the expected life, respectively. The random variable vector $\boldsymbol{X}$ includes external loads, material properties, crack geometry (initial position, initial crack angle, and crack position).

The FPI method, one of the most used recently, can be thought of as an extension to the Hasofer-Lind formulation[8] which starts with the transformations

$$u_i = (X_i - \mu_i)/\sigma_i \tag{3}$$

Here u_i is the reduced variable, and μ_i and σ_i are the mean and standard deviation of X_i, respectively. By substitution, $g(\boldsymbol{X})$ can be expressed as $g(\boldsymbol{u})$ in terms of reduced variable u_i. Then, the reliability index β is defined as the minimum distance from the origin of the reduced coordinates to the limit state. The probability of failure is given by

$$p_f = \Phi(-\beta) \tag{4}$$

where Φ is the standard normal cumulative distribution function.

$N(\boldsymbol{X})$ usually is an implicit function of random vector $\boldsymbol{X}$. It is difficult to obtain a closed form of $N(\boldsymbol{X})$ for real structures. Expanding it by Taylor's series expansion at the median values of X_i, or equivalently, at $u_i = 0$, we have

$$N(u) = N|_{u=0} + \sum_{i=1}^{n} \left(\frac{\partial N}{\partial X_i}\right)\left(\frac{\partial X_i}{\partial u_i}\right)\Bigg|_{u=0} (u_i - 0) + \text{HOT} \tag{5}$$

One can retain the higher order terms (HOT) of Taylor's series to estimate higher moments of $N(u)$. By selecting a set of data points u_i and calculating corresponding values $N_i(u)$, we can get the coefficients in the Taylor's series. Now the performance function can be approximated as a polynomial function.

Crack Growth Laws

The most common law for fatigue crack growth is the Paris-Erdogan law[10]

$$\frac{da}{dN} = C\{\Delta K(a)_{eq}\}^n \tag{6}$$

or its alternate form

$$\int_0^N dN = \int_{a_i}^{a_f} \frac{da}{C\{\Delta K(a)_{eq}\}^n} \tag{7}$$

where C and n are material properties. $\Delta K(a)_{eq}$ is the range of equivalent mode I stress intensity factor.

$$\Delta K(a)_{eq} = K_{eq}^{max} - K_{eq}^{min} \tag{8}$$

K_{eq}^{max} and K_{eq}^{min} are the maximum and minimum equivalent mode I stress intensity factors associated with the maximum and minimum cyclic applied stress.

By the maximum principal stress theory,[11] the $\Delta K(a)_{eq}$ can be expressed as

$$\Delta K(a)_{eq} = \Delta K_I \cos^3\frac{\theta_0}{2} - 3\Delta K_{II}\cos^2\frac{\theta_0}{2}\sin\frac{\theta_0}{2} \tag{9}$$

where θ_0 is the angle between the previous and current crack propagation direction.

There are several criteria for determining crack growth direction for mixed-mode fracture. Three of the most widely accepted are 1) the minimum strain energy density theory which states that crack initiation will start in a radial direction along which the strain energy density is a minimum; 2) the maximum energy release rate theory which states that the crack will extend in the direction along which the elastic energy release rate will be maximum, and the crack will start to grow when this energy release rate reaches a critical value; and 3) the maximum circumferential stress theory developed by Erdogan and Sih,[11] which states that the crack will start to grow from the crack tip in the direction along which the tangential stress is maximum and the shear stress is zero, i.e.,

$$\cos\theta/2[K_I \sin\theta + K_{II}(3\cos\theta - 1)] = 0 \tag{10}$$

which yields

$$K_I \sin\theta + K_{II}(3\cos\theta - 1) = 0 \tag{11}$$

or

$$\cos\theta/2 = 0 \tag{12}$$

Equation (12) indicates $\theta = \pm\pi$ which are the free surface directions of the fatigue crack. Equation (11) provides the relations between θ, K_I and K_{II}, which can be used to calculate the crack propagation direction. In the Appendix, it is shown that Eq. (11) can be also obtained from minimum potential energy criterion.

To evaluate the service life $N(u)$, the stress intensity factors must be known. These stress intensity factors can be determined analytically or by experimental testing only for simple structures.[12] In general they have to be evaluated by numerical techniques such as the finite element method.

The stress concentration near the crack tip area can be simulated either by regular finite elements which usually require a very substantial refinement in the vicinity of the crack tip or by fewer numbers of so-called singular elements in which the stress/strain singularity is implemented by predesigned shape functions. It is quite expensive in computer time and data preparation efforts to use these refined meshes, especially in the problem of probabilistic structural analysis. Thus, in the present study the singular finite element approach is suggested, and the stress intensity factors are obtained from the near-tip displacement field.[13,14]

New Methodology of Fatigue Crack Growth Reliability

According to Eq. (7), the service life is a function of the material properties, the stress intensity factor, and the crack path. However, the crack path along which the crack propagates is dependent on the primary random variables. Therefore, to evaluate the fatigue crack growth reliability, the crack path must be determined before performing the reliability analysis.

As mentioned before, for mode I fatigue problems, straight crack growth is expected. However, for the mixed-mode problem the crack path is a curve. It is implied that the crack propagation direction varies during its growth. Even at the same initial crack location with different set values of primary random variables, the crack propagation directions are different. This, in turn, jeopardizes the fatigue crack growth reliability analysis which requires, as it is stated before, a predefined crack path.

In this research a new method is proposed to determine the crack path of a structure under mixed-mode (mode I and mode II) fatigue loading. The idea is to divide the entire crack path into many segments. In each segment, the curved crack path is approximated by a polynominal function such as

$$y = c_0 + c_1 x + c_2 x^2 + , \ldots , c_k x^k = \sum_{i=0}^{k} c_i x^i \tag{13}$$

if a plane problem is considered. Once the coefficients $c_i (i = 0, \ldots, n)$ are found, the curve of this segment can be determined under this set of values of random variables. Obviously c_i are dependent on the primary random variables (external loads, material properties, ...). To simplify the problem, a quadratic function to describe each segment of a crack path is suggested. Because the length of each segment can be relatively small, the quadratic approximation is considered sufficient, i.e.,

$$y = c_0 + c_1 x + c_2 x^2 \tag{14}$$

According to Eq. (14), the service life (N) is not only related to the primary random variables but also is dependent on the crack path (y) defined by the unknown coefficients (c_0, c_1, c_2) of each segment, i.e.,

$$N = N(b, c) \tag{15}$$

In which b is the primary random variables and $\mathbf{c}$ represents the unknown coefficients.

Now let us assume that the current crack tip is located at (x_i, y_i) and the following crack tip position is (x_{i+1}, y_{i+1}). Hence, at the point(x_i, y_i), the assumed polynominal function should satisfy

$$y(x_i) = y_i \tag{16}$$

and

$$y'(x_i) = \tan \theta_i \tag{17}$$

The angle θ_i is determined by Eq. (11). According to the discussion in the Appendix, at the point (x_{i+1}, y_{i+1}), the crack direction law, Eq. (11), should also be satisfied. However, the point (x_{i+1}, y_{i+1}) has not been determined yet. It can be defined if coefficients c_0, c_1, and c_2 are known. In this study, an iterative method is presented to calculate these coefficients via the following procedure:

1) Assume an arbitrary value for any one of these three coefficients, for example, c_1.

2) The other two unknown coefficients can be calculated through Eqs. (16) and (17).

3) Based on this segment crack path, remesh the elements, and analyze the structure.

4) Calculate the stress intensity factors corresponding to the updated crack path, and then the crack direction θ_{i+1} at point (x_{i+1}, y_{i+1}) can be obtained by using the crack direction law.

5) Substitute θ_{i+1} into Eq. (17), c_1 can be solved.

6) Go to step 2, repeat this procedure until convergence is reached.

Table 1 Problem data (mode I)

Parameter	Distribution	Mean	Standard deviation	%
Length L	Deterministic	20.0 in.	0.0	0.0
Width W	Deterministic	4.0 in.	0.0	0.0
Thickness t	Deterministic	1.0 in.	0.0	0.0
Young's modulus E	Deterministic	$3.0E+7$	0.0	0.0
Poisson's ratio ν	Deterministic	0.3	0.0	0.0
Tension load σ	Normal	$1.2E+4$	$1.2E+3$	10
Initial crack length a_i	Lognormal	0.01 in.	0.001 in.	10
Fatigue parameter C	Normal	$1.0E-10$	$3.0E-11$	30
Fatigue parameter n	Normal	3.25	0.08	2.5

With the predicted crack propagation curve, the service life for this segment of crack curve can be obtained through the Paris-Erdogan law which, in this research, is expressed as

$$\Delta N = \int_{a_i}^{a_{i+1}} \frac{1}{C\{\Delta K(a)_{\text{eq}}\}^n} da = \int_{x_i}^{x_{i+1}} \frac{1}{C\{\Delta K(a)_{\text{eq}}\}^n} \sqrt{1 + (y')^2}\, dx \tag{18}$$

One can observe that the crack path is sensitive to the variables such as loading, material properties, and initial crack geometry which usually cannot be defined precisely in most practical problems. Therefore, considering the effects of the uncertainty of those variables, the reliability is calculated through a probabilistic structural analysis process using the NESSUS/FPI module. The entire analysis process is described as follows.

1) Determine the initial crack tip location, say (x_0, y_0).

2) According to the distributions of random variables, choose a set of values of random variables; under these values calculate the crack path by the proposed iterative procedure.

3) Obtain the stress intensity factors, crack length, and service life.

4) Change the values of random variables, calculate another crack path and corresponding service life.

5) Calculate the reliability of the structure through NESSUS/FPI.

6) Move to the next segment and repeat steps 2–5.

Examples and Discussions

In this study, two fatigue crack growth reliability analyses are performed: mode I and mixed-mode fatigue crack growth reliability problems. In these two examples, initial crack length, external tensile force and shear force, and crack growth parameters C and n in the Paris-Erdogan law are considered as primary random variables. To simplify the problem, other variables, such as structural configuration, crack position, crack orientation, etc. are assumed determinates. The system uncertainties in the fatigue crack growth problem now can be expressed as

$$b = [a_i, \sigma, \tau, C, n] \tag{19}$$

where a_i is the initial crack length. In the mixed-mode, a_i is considered to be deterministic and σ and τ are applied tensile and shear loads, respectively. C and n are parameters in the crack growth law. For the mode I shear stress τ is zero.

Reliability for the Mode I Fatigue Growth

The methodology has been applied to a through-the-thickness single-edge cracked plate under a uniform distributed tensile load as shown in Fig. 1.

The mean value of external load which is normally distributed is 12 ksi. Because of the symmetries of structure and external load, only the upper-half is considered. The problem data are tabulated in Table 1. Figure 2 is the stress intensity factors vs crack length. The solid curve is the solution from the deterministic finite element method (FEM), and the dashed curve represents the predictions based on Ref. 12. One can observe that these results are in good agreement, and the difference is less than 1% when the crack grows from 0.01 in. to 0.1 in.

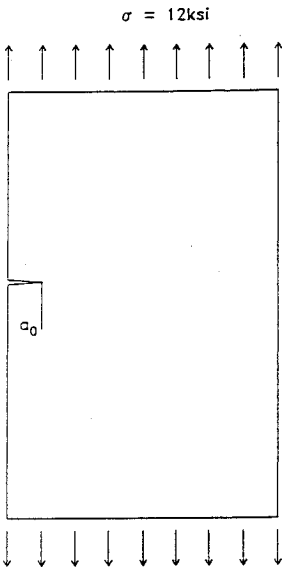

Fig. 1 Model for mode I crack problem.

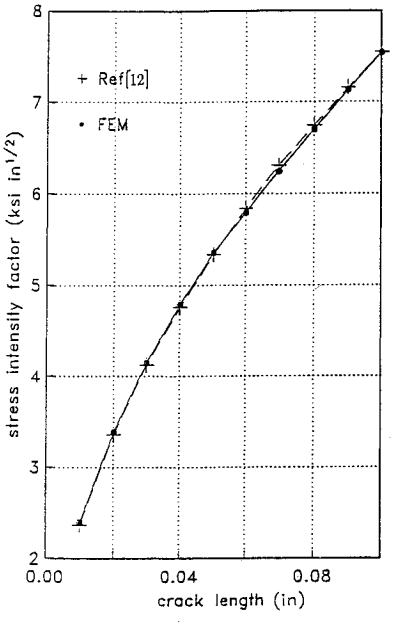

Fig. 2 Comparison of the mode I stress intensity factors during crack propagation between Ref. 12 and FEM solutions.

The fatigue lives vs crack length are depicted in Fig. 3. It is shown in the figure that at least $3.3E + 6$ cycles is needed for the crack to propagate from 0.01 in. to 0.02 in. However, it takes only about an additional $3.88E + 6$ cycles for the crack to grow from 0.02 in. to 0.1 in. It needs to be mentioned here that in Figs. 3 and 4 dashed curves are based on the stress intensity factor values provided by Ref. 12. One can see in Fig. 3 and in following Fig. 4 that the relative difference between the results is bigger than in Fig. 2. This can be explained by observing Eq. (18), when the exponent of $\Delta K(a)_{eq}$ n is over 3, the small error in stress intensity factor can induce a bigger error.

The comparison of combined effect under the effects of all uncertainties listed in Table 1 between the solutions based on the handbook[12] and the present finite element predictions is shown in Fig. 4. The results are presented in terms of cumulative probability vs fatigue life. The x axis is the fatigue life when the crack propagates from 0.01 in. to 0.1 in., and the vertical axis is the cumulative probability. It is important to note that a small error in stress intensity factor can induce a bigger error in fatigue life and even bigger in cumulative probability.

Reliability for the Mixed-Mode Fatigue Growth

The methodology has been also applied to a through-the-thickness single-edge cracked plate under uniformly distributed shear and tensile loads as shown in Fig. 5. The mean values of external shear and tensile force are 12 ksi and the initial crack length a_i is 0.1 in. Other random variables are listed in Table 2. Since the curved crack path destroys the symmetry of the problem, in this case, the entire plate will be meshed to analyze the crack propagation and evaluate the reliability of structure. The analyses for mixed mode are much more involved than for the mode I crack propagation problem.

By the proposed iterative procedure described in the previous section, the expressions for each crack segment under every set values of random variables are obtained. For example, when the increment of crack from initial crack tip in the x direction is 0.05 in., the corresponding predicted crack curve function is

$$y = 10.14147 - 1.40143x - 0.1316x^2 \tag{20}$$

In Fig. 6, a complete crack path propagated from $x = 0.1$ in. to $x = 0.4$ in. is shown under the mean values of external loads. Only part of the model near the crack tip is presented in Fig. 6.

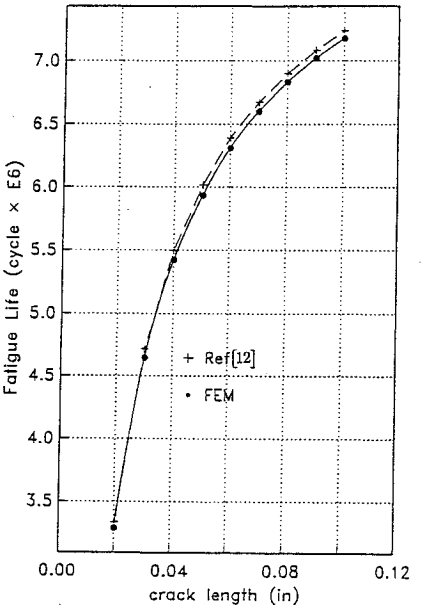

Fig. 3 Comparison of fatigue life during crack propagation between Ref. 12 and FEM solutions.

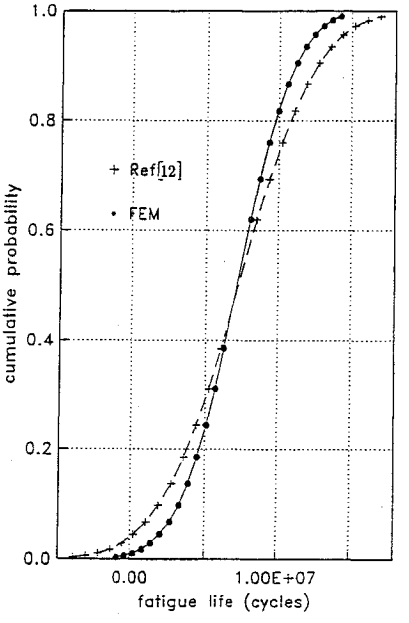

Fig. 4 Comparison of combined effect under effects of all uncertainties listed in Table 1 between Ref. 12 and FEM solutions.

Table 2 Problem data (mixed-mode)

Parameter	Distribution	Mean	Standard deviation	%
Length L	Deterministic	20.0 in.	0.0	0.0
Width W	Deterministic	4.0 in.	0.0	0.0
Thickness t	Deterministic	1.0 in.	0.0	0.0
Initial crack length a_i	Deterministic	0.1 in.	0.0	0.0
Young's modulus E	Deterministic	$3.0E+7$	0.0	0.0
Poisson's ratio ν	Deterministic	0.3	0.0	0.0
Tension load σ	Normal	$1.2E+4$	$1.2E+3$	10
Shear stress τ	Normal	$1.2E+4$	$1.2E+3$	10
Fatigue parameter C	Normal	$1.0E-10$	$3.0E-11$	30
Fatigue parameter n	Normal	3.25	0.08	2.5

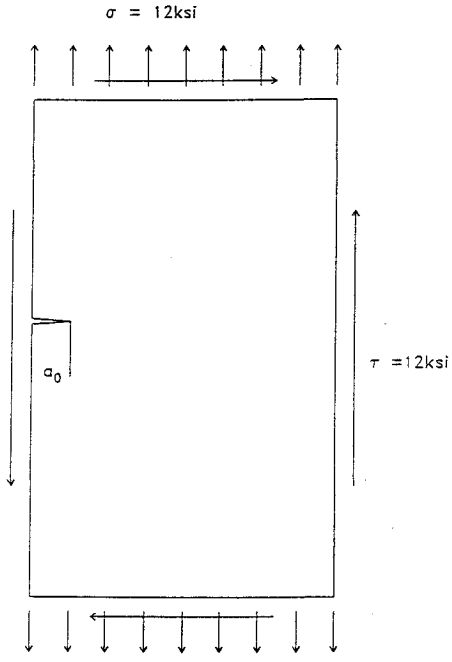

Fig. 5 Model of mixed-mode crack problem.

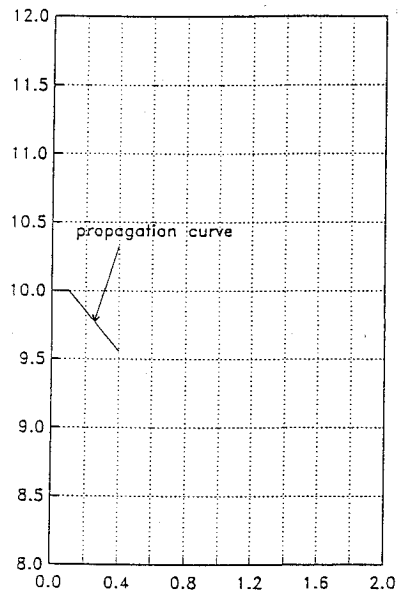

Fig. 6 Mixed-mode crack propagation curve.

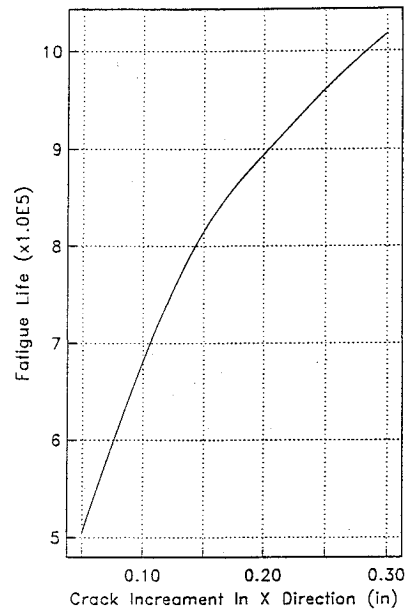

Fig. 7 Relationship between fatigue life and crack increment in x direction for mean values of random variables.

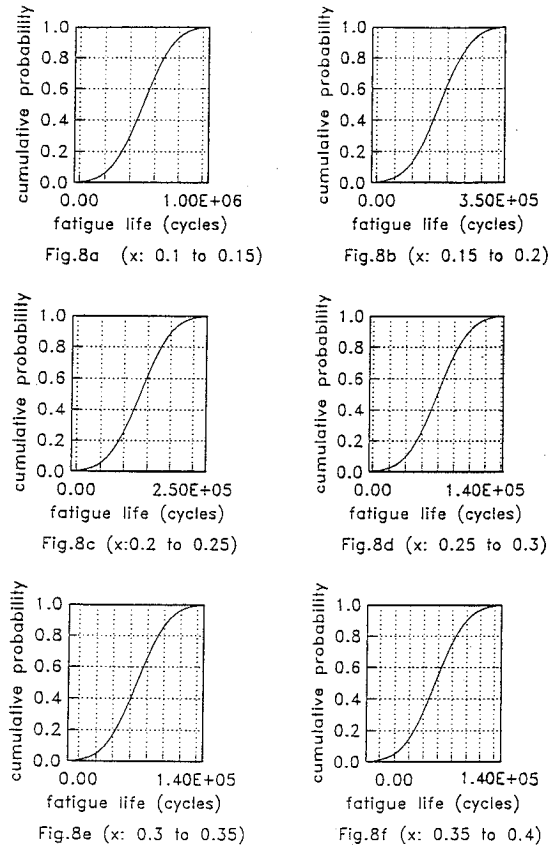

Fig. 8 Cumulative probabilities for each segment.

Under the mean values of random variables the relationship between fatigue life and crack increment in the x direction is obtained and shown in Fig. 7. It is interesting to note that the increasing rate of the fatigue life is getting smaller when the crack propagated. For instance, when the crack increment in the x direction from initial crack tip is 0.05 in., the fatigue life increases about 5.0×10^5. However, it takes almost the same number of life cycles for the crack to propagate an additional 0.3 in. (from $x = 0.1$ in. to 0.4 in.). This tendency is similar to that which was observed in the mode I fatigue crack problem.

Figure 8 shows the cumulative probabilities for six propagating periods. Under each figure, the caption ($x : x_1$–x_2) indicates that the

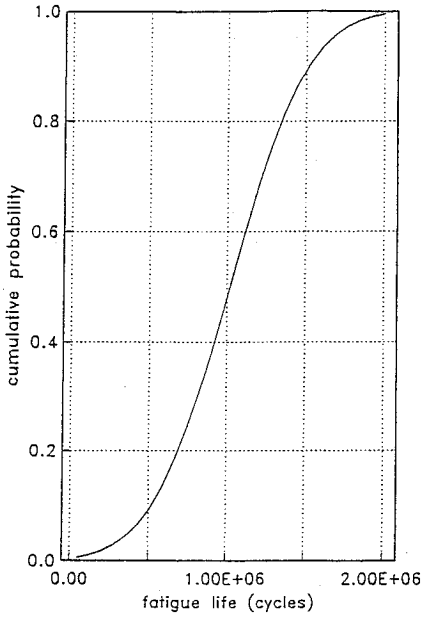

Fig. 9 Cumulative probability for whole crack path.

crack propagates in the x direction from x_1 to x_2. For example, Fig. 8a shows the probability of failure for crack propagation from $x = 0.1$ in. to $x = 0.15$ in. The deterministic fatigue life for this period is 5.05×10^5. When a 99% reliability is chosen, the service life will be 4.6×10^4. In the actual design, the requirement on reliability usually is higher than 99%. Consequently, the actual service life is much less than the deterministic fatigue life.

The cumulative probability of failure for the entire crack path, a total of six crack path periods, is shown in Fig. 9. The deterministic fatigue life cycles are 1.018×10^6. When the fatigue life reaches 2×10^6 the failure probability is over 99%. Finally, in this study, the sensitivity analysis of random variables is also carried out for different failure probability levels. For example, the most two sensitive variables at 0.99 probability level are determined to be the fatigue material properties n and C where the corresponding sensitivity factors are 0.539 and 0.783, respectively. That means at this level C is more sensitive.

Appendix

A. Potential Energy of a Cracked Body

The two elastic bodies shown in Figs. A1 and A2 are under the action of the same prescribed surface tractions T_i on S_T. They are otherwise identical except that the crack in the second body has propagated a farther length $2s$. Both bodies can be envisioned as having a crack of length $a_0 + 2s$ except that the crack of the first body is closed by an amount $2s$ by stress $\sigma_{si}^{(2s)}$ acting on the crack surfaces over $2s$. In this case, the stress component $\sigma_{si}^{(2s)}$ of the first body on $2s$ should be included as part of the tractions of the first body. Thus, in the absence of body forces, Betti's reciprocal theorem, which states that for a linear elastic body subjected to two different loadings the work done by the first loading acting through the displacements produced by the second loading equals the work done by the second loading acting through the displacements due to first loading, yields

$$\int_{S_T} T_i^{(1)} u_i^{(2)}\,ds + \int_{2s} \sigma_{si}^{(2s)} [u_i^- - u_i^+]\,ds = \int_{S_T} T_i^{(2)} u_i^{(1)}\,ds \quad \text{(A1)}$$

Here, $T_i^{(1)}$ and $T_i^{(2)}$ are the prescribed tractions on the S_T for two bodies. They are the same and equal to T_i. S_T represents the prescribed traction boundary. The $u_i^{(1)}$ and $u_i^{(2)}$ are the displacement fields of the first and the second body and u_i^- and u_i^+ stand for displacements at the lower and upper crack faces of second body over crack extension $2s$, respectively.

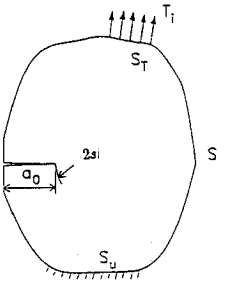

Fig. A1 A cracked plan body with an initial fatigue crack.

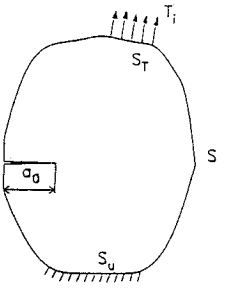

Fig. A2 The crack propagates additional length $2s$ from the initial crack tip.

According to Clapeyron's theorem, the potential energies of the first and second body are

$$\Pi_{(1)} = -\frac{1}{2}\int_{S_T} T_i u_i^{(1)}\,ds \quad \text{(A2)}$$

and

$$\Pi_{(2)} = -\frac{1}{2}\int_{S_T} T_i u_i^{(2)}\,ds, \quad \text{(A3)}$$

respectively. Then the potential energy release (the variation of potential energy) between the bodies is

$$\Delta\Pi = \Pi_{(2)} - \Pi_{(1)} \quad \text{(A4)}$$

Substituting Eqs. (A1–A3) into (A4), we have

$$\Delta\Pi = -\frac{1}{2}\int_{2s} \sigma_{si}^{(2s)} [u_i^+ - u_i^-]\,ds \quad \text{(A5)}$$

Thus, the potential energy of the second body can be formulated by adding the potential energy release due to the crack extension to the first body's potential energy,

$$\Pi_{(2)} = \Pi_{(1)} + \Delta\Pi \quad \text{(A6)}$$

As was stated in the previous section, the basic idea of our approach is that the direction of crack propagation minimizes the potential energy of the cracked body. In other words, the first derivative of $\Pi_{(2)}$ with respect to θ is zero. This implies that

$$\frac{\partial\Pi_{(2)}}{\partial\theta} = \frac{\partial\Pi_{(1)}}{\partial\theta} + \frac{\partial\Delta\Pi}{\partial\theta} = 0 \quad \text{(A7)}$$

Since Π_1 is independent of θ, the equation becomes

$$\frac{\partial\Pi_{(2)}}{\partial\theta} = \frac{\partial\Delta\Pi}{\partial\theta} = 0 \quad \text{(A8)}$$

Following the procedure described in the crack growth reliability section, the crack path is divided in m segments. Thus, the maximum energy release can be expressed as a summation of the maximum energy releases from these crack of segments,

$$\Delta\Pi = \Delta\Pi_1 + \Delta\Pi_2 + \Delta\Pi_3 + \cdots + \Delta\Pi_m = \sum_{i=1}^{m} \Delta\Pi_i \quad \text{(A9)}$$

Substituting Eq. (A9) into Eq. (A8), we obtain

$$\frac{\partial \Delta\Pi}{\partial\theta} = \frac{\partial \Delta\Pi_1}{\partial\theta} + \frac{\partial \Delta\Pi_2}{\partial\theta} + \frac{\partial \Delta\Pi_3}{\partial\theta} + \cdots + \frac{\partial \Delta\Pi_m}{\partial\theta}$$

$$= \sum_{i=1}^{m} \frac{\partial \Delta\Pi_i}{\partial\theta} = 0 \tag{A10}$$

Since the derivations of the preceding equation are independent, it indicates that each term must equal zero. This leads to

$$\left.\frac{\partial \Delta\Pi_1}{\partial\theta}\right|_{\theta_1} = 0$$

$$\left.\frac{\partial \Delta\Pi_2}{\partial\theta}\right|_{\theta_2} = 0$$

$$\left.\frac{\partial \Delta\Pi_3}{\partial\theta}\right|_{\theta_3} = 0$$

$$\cdots$$

$$\left.\frac{\partial \Delta\Pi_m}{\partial\theta}\right|_{\theta_m} = 0 \tag{A11}$$

where $\theta_1, \theta_2, \ldots, \theta_m$ are the crack growth directions of segments $1, 2, \ldots, m$, respectively.

A description of the direction of crack propagation can thus be formulated by substituting an explicit form of the variation of potential energies $\Delta\Pi_i$ due to the crack extension into Eq. (A11).

B. Potential Energy Release (ΔPi_i)

The coordinate systems at the crack tip are defined in Fig. A3, in which the origin of the x and y coordinates is located at the initial crack tip. Let x^i of coordinate system x^i, y^i be along the direction of crack propagation θ_i. Hence, x^1 is defined to be the direction along the direction of propagation θ_1. According to linear fracture mechanics, for a plane loading problem, the stress components in terms of r, the distance from the end of segment 1, and θ, are

$$\sigma_x = \frac{K_{\mathrm{II}}}{\sqrt{2\pi r}} \cos\frac{\theta}{2}\left[1 - \sin\frac{\theta}{2}\sin\left(\frac{3\theta}{2}\right)\right]$$

$$+ \frac{K_{\mathrm{III}}}{\sqrt{2\pi r}}\left(-\sin\frac{\theta}{2}\right)\left[2 + \cos\frac{\theta}{2}\cos\frac{3\theta}{2}\right] \tag{A12}$$

$$\sigma_y = \frac{K_{\mathrm{II}}}{\sqrt{2\pi r}} \cos\frac{\theta}{2}\left[1 + \sin\frac{\theta}{2}\sin\left(\frac{3\theta}{2}\right)\right]$$

$$+ \frac{K_{\mathrm{III}}}{\sqrt{2\pi r}} \sin\frac{\theta}{2}\cos\frac{\theta}{2}\cos\frac{3\theta}{2} \tag{A13}$$

$$\tau_{xy} = \frac{K_{\mathrm{II}}}{\sqrt{2\pi r}} \cos\frac{\theta}{2}\sin\frac{\theta}{2}\cos\left(\frac{3\theta}{2}\right)$$

$$+ \frac{K_{\mathrm{III}}}{\sqrt{2\pi r}} \cos\frac{\theta}{2}\left[1 - \sin\frac{\theta}{2}\sin\frac{3\theta}{2}\right] \tag{A14}$$

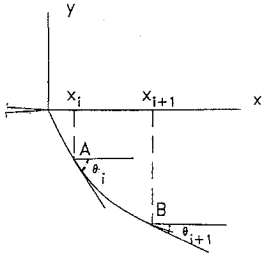

Fig. A3 Coordinate systems along the crack extension path.

where K_{II} and K_{III} are the stress intensity factors corresponding to the initial crack tip of segment 1. By the transformation, the stress components in coordinate system x^1, y^1 are

$$\sigma_{x^1} = \frac{K_{\mathrm{II}}}{\sqrt{2\pi r}} \cos\frac{\theta}{2}\left[1 + \sin^2\frac{\theta}{2}\right] + \frac{K_{\mathrm{III}}}{\sqrt{2\pi r}}$$

$$\times\left[-\sin\frac{\theta}{2} + \sin\frac{3\theta}{2} - \sin\frac{\theta}{2}\left(\cos\frac{\theta}{2}\right)^2\right] \tag{A15}$$

$$\sigma_{y^1} = \frac{K_{\mathrm{II}}}{\sqrt{2\pi r}} \cos^3\frac{\theta}{2} + \frac{K_{\mathrm{III}}}{\sqrt{2\pi r}}\left[-\sin\frac{\theta}{2} - \sin\frac{3\theta}{2}\right.$$

$$\left. + \sin\frac{\theta}{2}\left(\cos\frac{\theta}{2}\right)^2\right] \tag{A16}$$

$$\tau_{x^1y^1} = \frac{K_{\mathrm{II}}}{\sqrt{2\pi r}}\left(\cos\frac{\theta}{2}\right)^2 \sin\frac{\theta}{2} + \frac{K_{\mathrm{III}}}{\sqrt{2\pi r}}$$

$$\times\left[\left(\sin\frac{\theta}{2}\right)^2 \cos\frac{\theta}{2} + \cos\frac{3\theta}{2}\right] \tag{A17}$$

Suppose the crack extends a length $2\Delta s$ in segment 1, where Δs is equal to s/m if each segment has the same length. According to Ref. 15, the mode I stress intensity factor corresponding to the initial crack tip of segment 2 can be expressed as a closed form as

$$K_{\mathrm{I2}}(a_0 + 2\Delta s) = \frac{1}{\sqrt{\pi\,\Delta s}} \int_{-\Delta s}^{\Delta s} \left(\frac{\Delta s + t}{\Delta s - t}\right)^{\frac{1}{2}} p_2(t)\,\mathrm{d}t \tag{A18}$$

where $p_2(t)$ is the tensile stress component

$$p_2(t) = \frac{K_{\mathrm{II}}}{\sqrt{2\pi(\Delta s + t)}} \cos^3\frac{\theta}{2} + \frac{K_{\mathrm{III}}}{\sqrt{2\pi(\Delta s + t)}}$$

$$\times\left[-\sin\frac{\theta}{2} - \sin\frac{3\theta}{2} + \sin\frac{\theta}{2}\left(\cos\frac{\theta}{2}\right)^2\right] \tag{A19}$$

Therefore, substituting Eq. (A19) into Eq. (A18) and integrating it over $(-\Delta s, \Delta s)$, we have

$$K_{\mathrm{I2}}(a_0 + 2\Delta s) = \frac{2}{\pi} K_{\mathrm{II}} \cos^3\frac{\theta}{2} + \frac{2}{\pi} K_{\mathrm{III}}$$

$$\times\left[-\sin\frac{\theta}{2} - \sin\frac{3\theta}{2} + \sin\frac{\theta}{2}\left(\cos\frac{\theta}{2}\right)^2\right] \tag{A20}$$

Similarly, the stress intensity factor of mode II is

$$K_{\mathrm{II2}}(a_0 + 2\Delta s) = \frac{1}{\sqrt{\pi\,\Delta s}} \int_{-\Delta s}^{\Delta s} \left(\frac{\Delta s + t}{\Delta s - t}\right)^{\frac{1}{2}} p_1(t)\,\mathrm{d}t \tag{A21}$$

and $p_1(t)$ is the shear stress

$$p_1(t) = \frac{K_{\mathrm{II}}}{\sqrt{2\pi(\Delta s + t)}}\left(\cos\frac{\theta}{2}\right)^2 \sin\frac{\theta}{2}$$

$$+ \frac{K_{\mathrm{III}}}{\sqrt{2\pi(\Delta s + t)}}\left[\left(\sin\frac{\theta}{2}\right)^2 \cos\frac{\theta}{2} + \cos\frac{3\theta}{2}\right] \tag{A22}$$

Hence, by substituting Eq. (A22) into Eq. (A21) and integrating it over $(-\Delta s, \Delta s)$, we have

$$K_{\mathrm{II2}}(a_0 + 2\Delta s) = \frac{2}{\pi} K_{\mathrm{II}}\left(\cos\frac{\theta}{2}\right)^2 \sin\frac{\theta}{2}$$

$$+ \frac{2}{\pi} K_{\mathrm{III}}\left[\left(\sin\frac{\theta}{2}\right)^2 \cos\frac{\theta}{2} + \cos\frac{3\theta}{2}\right] \tag{A23}$$

For a plane problem, the general expressions of displacement components are

$$u_1 = \frac{K_{II}}{2\mu}\sqrt{\frac{r}{2\pi}}\cos\frac{\theta}{2}\left[k-1+2\sin^2\frac{\theta}{2}\right] + \frac{K_{III}}{2\mu}\sqrt{\frac{r}{2\pi}}\sin\frac{\theta}{2}\left[k+1+2\cos^2\frac{\theta}{2}\right] \quad \text{(A24)}$$

$$u_2 = \frac{K_{II}}{2\mu}\sqrt{\frac{r}{2\pi}}\sin\frac{\theta}{2}\left[k+1-2\cos^2\frac{\theta}{2}\right] + \frac{K_{III}}{2\mu}\sqrt{\frac{r}{2\pi}}\left(-\cos\frac{\theta}{2}\right)\left[k-1-2\sin^2\frac{\theta}{2}\right] \quad \text{(A25)}$$

In (A24) and (A25), μ is shear modulus and k is defined as

$$k = \begin{cases} \frac{3-\nu}{1+\nu} & \text{for plane stress} \\ 3-4\nu & \text{for plane strain} \end{cases}$$

where ν is Poisson's ratio. When the crack extends to the end of the first segment (x_2, y_2), the displacements at the upper crack face are obtained by substituting $\theta = \pi$ into Eqs. (A24) and (A25). They are

$$u_1^+(a_0+2\Delta s) = \frac{K_{III}(a_0+2\Delta s)}{2\mu}\left(\frac{2\Delta s - r}{2\pi}\right)^{\frac{1}{2}}(k+1) \quad \text{(A26)}$$

$$u_2^+(a_0+2\Delta s) = \frac{K_{II}(a_0+2\Delta s)}{2\mu}\left(\frac{2\Delta s - r}{2\pi}\right)^{\frac{1}{2}}(k+1) \quad \text{(A27)}$$

where r is the distance from the initial crack tip. Similarly, by substituting $\theta = -\pi$ into Eqs. (A24) and (A25), the displacements at lower crack are

$$u_1^-(a_0+2\Delta s) = -\frac{K_{III}(a_0+2\Delta s)}{2\mu}\left(\frac{2\Delta s - r}{2\pi}\right)^{\frac{1}{2}}(k+1) \quad \text{(A28)}$$

$$u_2^-(a_0+2\Delta s) = -\frac{K_{II}(a_0+2\Delta s)}{2\mu}\left(\frac{2\Delta s - r}{2\pi}\right)^{\frac{1}{2}}(k+1) \quad \text{(A29)}$$

Comparing Eqs. (A26) and (A27) with Eqs. (A28) and (A29), one finds at once

$$u_1^-(a_0+2\Delta s) = -u_1^+(a_0+2\Delta s) \quad \text{(A30)}$$

$$u_2^-(a_0+2\Delta s) = -u_2^+(a_0+2\Delta s) \quad \text{(A31)}$$

Substituting Eqs. (A30) and (A31) into Eq. (A5) and realizing that $\sigma_{si}^{(\Delta s)}$ are stresses acting on segment 1 without crack extension yields

$$-\Delta\Pi_1 = \int_0^{2\Delta s} u_1^+(a_0+2\Delta s)\tau_{x^1y^1}\,dr + \int_0^{2\Delta s} u_2^+(a_0+2\Delta s)\sigma_{y^1}\,dr \quad \text{(A32)}$$

Finally, upon substitution of Eqs. (A16), (A17), (A26), and (A27) into Eq. (A32), a closed form of the potential energy release for the first segment is obtained

$$-\Delta\Pi_1 = \frac{\Delta s(k+1)}{2\mu\pi}\left(\left[K_{II}\cos^3\frac{\theta}{2} + K_{III}\left(-\sin\frac{\theta}{2} - \sin\frac{3\theta}{2} + \sin\frac{\theta}{2}\left(\cos\frac{\theta}{2}\right)^2\right)\right]^2 + \left[K_{II}\cos^2\frac{\theta}{2}\sin\frac{\theta}{2} + K_{III}\left(\sin^2\frac{\theta}{2}\cos\frac{\theta}{2} + \cos\frac{3\theta}{2}\right)\right]^2\right) \quad \text{(A33)}$$

It is actually can be described as the change of potential energy due to the crack extension in the first segment.

For other segments, for example, segment i, conducting a similar procedure the potential energy release can be expressed as

$$-\Delta\Pi_i = \frac{\Delta s(k+1)}{2\mu\pi}\left\{\left[K_{Ii}\cos^3\frac{\theta}{2} + K_{IIi}\left(-\sin\frac{\theta}{2} - \sin\frac{3\theta}{2} + \sin\frac{\theta_i}{2}\left(\cos\frac{\theta}{2}\right)^2\right)\right]^2 + \left[K_{Ii}\cos^2\frac{\theta}{2}\sin\frac{\theta_i}{2} + K_{IIi}\left(\sin^2\frac{\theta}{2}\cos\frac{\theta}{2} + \cos\frac{3\theta}{2}\right)\right]^2\right\} \quad \text{(A34)}$$

where the stress intensity factors corresponding to the initial crack position at segment i are

$$K_{Ii}(a_0+2i\Delta s) = \frac{2}{\pi}K_{Ii}\cos^3\frac{\theta}{2} + \frac{2}{\pi}K_{IIi}\left[-\sin\frac{\theta}{2} - \sin\frac{3\theta}{2} + \sin\frac{\theta}{2}\left(\cos\frac{\theta}{2}\right)^2\right] \quad \text{(A35)}$$

and

$$K_{IIi}(a_0+2i\Delta s) = \frac{2}{\pi}K_{Ii}\left(\cos\frac{\theta}{2}\right)^2\sin\frac{\theta}{2} + \frac{2}{\pi}\times K_{IIi}\left[\left(\sin\frac{\theta}{2}\right)^2\cos\frac{\theta}{2} + \cos\frac{3\theta}{2}\right] \quad \text{(A36)}$$

C. Crack Growth Direction by Minimum Potential Energy

Substituting Eq. (A33) into the first formulation of Eq. (A11) after a tedious derivation, we have

$$\frac{\partial\Delta\Pi_1}{\partial\theta} = -\frac{s(k+1)}{4\mu\pi}[K_{II}\sin\theta + K_{III}(3\cos\theta - 1)] \times [-K_{II}(1+\cos\theta) + K_{III}\sin\theta]|_{\theta_1} = 0 \quad \text{(A37)}$$

For the case of mode I fracture, $K_{III} = 0$, then Eq. (A35) reduces to

$$\frac{\partial\Delta\Pi_1}{\partial\theta} = \frac{\Delta s(k+1)}{4\mu\pi}K_{II}^2\sin\theta(1+\cos\theta)|_{\theta_1} = 0 \quad \text{(A38)}$$

which leaves us with $\theta = 0$ or $\theta = \pm\pi$. This is the same results shown on the maximum stress criterion.[11]

For the case of a mode II fracture, $K_{II} = 0$, then

$$\frac{\partial\Delta\Pi_1}{\partial\theta} = -\frac{s(k+1)}{4\mu\pi}K_{III}^2\sin\theta_1(3\cos\theta - 1)|_{\theta_1} = 0 \quad \text{(A39)}$$

From which we can get $\sin\theta = 0$ or $(3\cos\theta - 1) = 0$. This solution again is the same with the prediction based on the maximum stress criterion.[11]

For the case of a mixed mode (mode I and II) fracture, Eq. (A37) gives

$$K_{II}\sin\theta + K_{III}(3\cos\theta - 1) = 0 \quad \text{(A40)}$$

or

$$-K_{II}(1+\cos\theta_1) + K_{III}\sin\theta_1 = 0 \quad \text{(A41)}$$

Again, for segment i, the minimization process implies

$$\frac{\partial\Delta\Pi_i}{\partial\theta} = -\frac{\Delta s(k+1)}{4\mu\pi}[K_{Ii}\sin\theta + K_{IIi}(3\cos\theta - 1)] = 0 \quad \text{(A42)}$$

which yields

$$K_{Ii}\sin\theta_i + K_{IIi}(3\cos\theta_i - 1) = 0 \quad \text{(A43)}$$

or

$$-K_{Ii}(1+\cos\theta_i) + K_{IIi}\sin\theta_i = 0 \quad \text{(A44)}$$

It is important to note that all the crack growth directions θ_i are defined with respect to the global coordinate system x, y where the origin is located at the initial crack tip of segment 1.

D. Summary

Equation (A40) and (A43) are the exact same form for the crack growth direction proposed by Erdogan and Sih[11] based on the hypothesis that the crack extension starts in the direction normal to that of the maximum tension stress. It is shown in this Appendix that the direction normal to the maximum tension stress minimizes the potential energy of the cracked body. In other words, the crack growth direction can also be obtained based on the principle of minimum potential energy.

Most importantly, in this Appendix we proved that the crack growth direction formulation Eq. (A12) can be applied to any portion of a continuous and smooth crack path.

Conclusions

A new methodology has been proposed for the prediction of the crack path and the evaluation of the cumulative probability of failure for mixed-mode crack propagation. Results have been shown to agree well with the predications based on Ref. 12. Even though the crack path was determined through a quarter-point finite element approach, the proposed methodology can be implemented by analytical as well as numerical analysis techniques. The methodology is a general approach and applicable to real structures.

Acknowledgment

The authors wish to acknowledge Christos Chamis of NASA Lewis Research Center for his encouragement in this research and for permission to use the NESSUS computer program.

References

[1]Chamis, C. C.,"Probabilistic Structural Analysis Methods for Space Propulsion System Components," NASA TM-88861, 1986.

[2]Wu, Y. T., and Wirsching, P. H.,"Advanced Reliability Method for Fatigue Analysis," *Journal of Engineering Mechanics*, Vol. 110, 1984, pp. 536–563.

[3]Shiao, M. C., and Chamis, C. C., "Probability of Failure and Risk Assessment of Propulsion Structural Components," *Proceedings of the JANNAF Propulsion Meeting*, Vol. 1, 1989, pp. 135–162.

[4]Millwater, H., Wu, Y. T., Torng, T., Thacker, B., Riha, D., and Leung, C. P., "Recent Development of The NESSUS Probabilistic Structural Analysis Computer Program", *Proceedings of AIAA/ASME/ASCE/AHS/ACS 34th Structures, Structural Dynamics and Materials Conference*, AIAA, Washington, DC, April 1993, pp. 614-624.

[5]Liu, W. K., Mani, A., and Belytschko, T.,"Finite Element Method in Probabilistic Mechanics," *Probabilistic Engineering Mechanics*, Vol. 2, 1988, pp. 201–213.

[6]Besterfield, G. H., Liu, W. K., Lawrence, M. A., and Belytschko, T., "Brittle Fracture Reliability by Probabilistic Finite Elements," *Journal of Engineering Mechanics*, Vol. 116, 1990, pp. 642–659.

[7]Besterfield, G. H., Liu, W. K., Lawrence, M. A., and Belytschko, T., "Fatigue Crack Growth Reliability by Probabilistic Finite Elements," *Computer Methods in Applied Mechanics and Engineering*, Vol. 86, 1991, pp. 297–320.

[8]Lua, Y. J., Liu, W. K., and Belytschko, T., "Curvilinear Fatigue Crack Reliability Analysis by Stochastic Boundary Element Method," *International Journal for Numerical Methods in Engineering*, Vol. 36, 1993, pp. 3841–3858.

[9]Lua, Y. J., Liu, W. K., and Belytschko, T., "Life Prediction of A Curvilinear Fatigue Crack Growth by SBIEM," *Reliability Technology*, AD-Vol. 28, edited by T. A. Cruse, 1992, pp. 99–111.

[10]Paris, P. C., and Erdogan, F., "A critical analysis of crack propagation laws," *Journal of Basic Engineering*, Vol. 85, 1963, pp. 528–534.

[11]Erdogan, F., and Sih, G. C., "On the Crack Extension in Plates Under Plane Loading and Transverse Shear," *Journal of Basic Engineering*, Vol. 85, 1963, pp. 519–527.

[12]Tada, H., *The Stress Analysis of Cracks Handbook* 2nd ed., 1985.

[13]Saouma, V. E., and Zatz, I. J., "An Automated Finite Element Procedure for Fatigue Crack Propagation Analysis," *Engineering Fracture Mechanics*, Vol. 20, 1984, pp. 321–333.

[14]Shih, C. F., DeLorenzi, H. G., and Andrews, W. R.,"Studies on Crack Initiation and Stable Crack Growth," *Elastic-Plastic Fracture Mechanics*, ASTM Special Technical Pub. No. 668, American Society for Testing and Materials, 1979, pp. 65–120.

[15]Kanninen, M. F., and Popelar, C. H., *Advanced Fracture Mechanics*, Oxford University Press, Oxford, England, UK, 1985.